



HAL
open science

The Saga of Water and Halide Perovskites: Evidence of Water in Methylammonium Lead Tri-Iodide

Naga Prathibha Jasti, Gennady E Shter, Yishay Feldman, Davide Raffaele Ceratti, Adi Kama, Isaac Buchine, Gideon S Grader, David Cahen

► **To cite this version:**

Naga Prathibha Jasti, Gennady E Shter, Yishay Feldman, Davide Raffaele Ceratti, Adi Kama, et al.. The Saga of Water and Halide Perovskites: Evidence of Water in Methylammonium Lead Tri-Iodide. *Advanced Functional Materials*, 2022, 32 (43), pp.2204283. 10.1002/adfm.202204283 . hal-04357952

HAL Id: hal-04357952

<https://hal.science/hal-04357952>

Submitted on 21 Dec 2023

HAL is a multi-disciplinary open access archive for the deposit and dissemination of scientific research documents, whether they are published or not. The documents may come from teaching and research institutions in France or abroad, or from public or private research centers.

L'archive ouverte pluridisciplinaire **HAL**, est destinée au dépôt et à la diffusion de documents scientifiques de niveau recherche, publiés ou non, émanant des établissements d'enseignement et de recherche français ou étrangers, des laboratoires publics ou privés.



Distributed under a Creative Commons Attribution 4.0 International License

The Saga of Water and Halide Perovskites: Evidence of Water in Methylammonium Lead Tri-Iodide

Naga Prathibha Jasti, Gennady E. Shter, Yishay (Isai) Feldman, Davide Raffaele Ceratti, Adi Kama, Isaac Buchine, Gideon S. Grader,* and David Cahen*

The environment humidity effects on performance of halide perovskites (HaPs), especially MAPbI₃, are known. Nevertheless, it is hard to find direct experimental evidence of H₂O in the bulk materials at the levels lower than that of Monohydrate (MAPbI₃·H₂O). Here, for the first time, direct experimental evidence of water being released from bulk (μm-s deep) of MAPbI₃ single crystal is reported. The thermogravimetric analysis coupled with mass spectrometry (TGA-MS) of evolved gases is used to detect the MS signal of H₂O from the penetrable depth and correlate it with the TGA mass loss due to H₂O leaving the material. These measurements yield an estimate of the average H₂O content of 1 H₂O molecule per three MAPbI₃ formula units (MAPbI₃·0.33H₂O). Under the relatively low temperature conditions no other evolved gases that can correspond to MAPbI₃ decomposition products, are observed in the MS. In addition to being direct evidence that there is H₂O inside MAPbI₃, the data show that H₂O diffuses into it. With this article, a solid basis is proved for further studies on the mechanisms through which water modifies the properties of MAPbI₃ and all the other halide perovskites.

optical properties.^[4–8] Leguy et al. reported reversible hydration of MAPI and that significant, irreversible water vapor-induced decomposition occurs only after a grain has been fully converted to the monohydrate phase.^[9] As there is a significant parameter space between the “low” and “high” humidity conditions, there is an active debate about how and how much water will be beneficial without pushing the material system into irreversible decomposition, including possible differences in rate and extent of effects of H₂O as vapor or liquid.

Earlier we demonstrated by Deuterium–Hydrogen exchange that water can drive proton diffusion in HaPs.^[10] This proton migration might influence the MAPI’s net defect density^[10,11] and can be related to its enhanced optoelectronic properties, when exposed to low water vapor densities.^[4] Optoelectronic effects on MAPI that occur


in the presence of H₂O, have been reported down to concentrations of 0.1 H₂O/MAPbI₃ formula unit,^[9] however, whether the H₂O is in the bulk, or at close to few monolayers, the surface, remains unanswered; it is also not clear if 0.1 H₂O/ MAPbI₃ suffices to cause proton migration and induce optoelectronic effects? So far, no direct experimental evidence points to H₂O in MAPI below the level of the monohydrate; in fact, computational theory has taken the lead in quantifying the energy required for H₂O to infiltrate into bulk MAPI.^[12,13] These latter

1. Introduction

High humidity (>70% RH) has been shown to be detrimental to the stability of halide perovskites (HaPs), especially Methylammonium Lead Iodide (MAPbI₃, MAPI)^[1–3] which is a promising semiconductor material for various applications. Lower humidity (≈40% RH), however, has been observed to play a key role in the crystallization of HaPs, apparent passivation of defects and, thus, enhancing its (opto)electronic and

N. P. Jasti, A. Kama, I. Buchine, D. Cahen
Inst. For Nanotechnol. & Adv. Mater., and Chem. Dept.
Bar Ilan University
Ramat Gan 5290002, Israel
E-mail: david.cahen@weizmann.ac.il

N. P. Jasti, D. R. Ceratti, D. Cahen
Department of Molecular Chemistry and Materials Science
Weizmann Institute of Science
Rehovot 7610001, Israel

 The ORCID identification number(s) for the author(s) of this article can be found under <https://doi.org/10.1002/adfm.202204283>.

© 2022 The Authors. Advanced Functional Materials published by Wiley-VCH GmbH. This is an open access article under the terms of the Creative Commons Attribution License, which permits use, distribution and reproduction in any medium, provided the original work is properly cited.

DOI: 10.1002/adfm.202204283

G. E. Shter, G. S. Grader
Dept. of Chemical Engineering
Technion – Israel Institute of Technology
Haifa 3200003, Israel
E-mail: grader@technion.ac.il

Y. (I.) Feldman
Department of Chemical Research Support
Weizmann Institute of Science
Rehovot 7610001, Israel

D. R. Ceratti
CNRS, UMR 9006, IPVF
Institut Photovoltaïque d’Ile-de-France
18 Boulevard Thomas Gobert, Palaiseau 91120, France

G. S. Grader
The Nancy & Stephen Grand Technion Energy Program (GTEP)
Technion – Israel Institute of Technology
Haifa 3200002, Israel

studies focus on possible mechanisms, and pathways that the H₂O could take, as well as the orientation of H₂O molecules inside the unit cell.^[14–18] Clearly, connecting the results of those studies to experimental observables, i.e., performing the experiments to check the results from model computations, is important. One principal question is to obtain as direct experimental evidence as possible for or against H₂O presence of, and diffusion into the bulk material.

We report here the effect of medium-high ambient humidity (≈50–65% RH) on MAPI single crystals using simultaneous differential and thermogravimetric analysis (TGA/DTA), coupled with mass spectrometry of evolved gases (MS), TGA/DTA-MS. While there are many reports that use TGA-MS to probe stability of perovskites in general and of MAPI, in particular, most of these reports used the technique to identify the decomposition temperature and the (release of its) decomposition products.^[19–21] Our interest is to directly detect the release of H₂O from bulk MAPI, under conditions where the MAPI crystal structure is intact. We present the first direct identification of the H₂O that is released from MAPI single crystals and importantly, that this occurs well below the temperature where thermal decomposition starts and from a depth, estimated at several tens of μm-s, at an average level below that of the lowest known hydrate, MAPbI₃·H₂O. This implies that H₂O molecules can diffuse into and from bulk MAPI. We finally discuss how the low concentration (corresponding to an average estimate, MAPbI₃·0.33H₂O) that we report can lead to the cited effects on diffusion and on the optoelectronic properties of the material, considering results on MAPI obtained by us^[10] and others.^[9] This is of interest as some exposure to humidity is realistically unavoidable in large-scale production of halide perovskite-based devices. Also, water exposure is a common issue when transferring perovskite samples to measurement instruments in most laboratories. In view of these practical considerations, the ability to choose measurement conditions for which information, such as what is provided here, is available, will allow to control conditions so that the samples' water content will have minimal effect on the experiment/production process.

2. Results and Discussion

Any surface effect or the existence of grain boundaries (possible capillary condensation between the grains) would interfere with our study on the intrinsic properties of MAPI. For this reason, we concentrated our attention on MAPI single crystals. We fabricated MAPI single crystals by Inverse Temperature Crystallization (Section I, Supporting Information). Unless specified otherwise, extracted, and vacuum-dried single crystals were stored in N₂, under a mild, continuous stream of N₂, at 9 ± 1% RH, 22.0 ± 0.5 °C. Phase-pure composition of the MAPI single crystals was verified by powder X-ray Diffraction (XRD) (Section II, Supporting Information), i.e., by measuring the pulverized single crystals (Figure S1, Supporting Information). The θ -2 θ (t - $2t$) XRD measurement shows peaks corresponding to the (100) crystallographic planes (Figure 1a) with a slight shift ($\Delta\theta = \approx 0.2^\circ$ for (400)) to lower angles, indicating a volume expansion of ≈1% for the unit cell. We also performed XRD Rocking Curve analysis around the $2\theta = 40.50^\circ$ (400) diffraction peak to assure the mono-crystallinity; a very small FWHM of 0.04° was observed (Figure 1b), confirming their high quality. Interestingly, while conserving the single-crystalline MAPI XRD structure, we observed an additional peak ≈8.07° in the θ -2 θ scan, corresponding to MAPbI₃·H₂O^[9] (001) crystallographic planes (crystal model shown in Figure S2, Supporting Information), possibly due to the crystal extraction conditions that were in ambient (mostly 50–60% RH, 25 °C). The higher order peaks corresponding to (002), (003), (004), and (006) reflections with very low relative intensity, which masked in linear scale, are observed at 2θ values 16.22°, 24.42°, 32.85°, and 50.12° respectively in square root scale (Figure S3, Supporting Information). Additionally, according to simulations, based on the powder diffraction database,^[22] the (001), (002), and (003) reflections should have almost the same intensities, while our data show the intensity of the (001) reflection to be much higher than those of the other two. From our result and based on the depths of Cu K α X-ray probing for Pb and I matrices for the (006) peak, at θ value ≈25.06°, it can

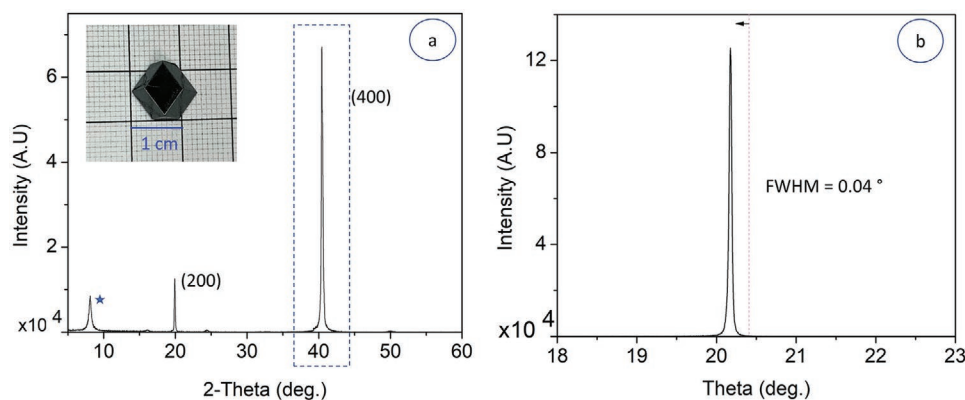


Figure 1. a) θ -2 θ XRD pattern for MAPbI₃; inset: photograph of the single crystal. The peak marked with the dotted rectangle is the diffraction angle (40.50°), at which the rocking curve, RC, is recorded; the peak marked with * fits the (001) diffraction of MAPbI₃·H₂O (and is in a range of 2θ values for Cu K α XRD), devoid of diffraction peaks from MAPI. The inset shows an actual MAPI crystal (cf. to a schematic representation in Figure S13, Supporting Information) b. RC scan at 2θ (40.50°) (the pink dashed line indicates the peak's theta position from the crystallographic information database and the arrow indicates the direction of the peak's shift for that of sample) Note: This theta shift is marked in the RC pattern, because of the high resolution of that plot.

be assumed that the thickness of the ordered monohydrate layer is $\approx 2 \mu\text{m}$. However, because in-diffusion from a surface yields a gradient of decreasing concentration of the diffusing species (H_2O , in our case) with depth, it is likely that disordered clusters of $\text{MAPbI}_3 \cdot \text{H}_2\text{O}$ and, ultimately isolated units will be found at greater depths. The results of the ϕ -scan for the (402) MAPI reflection under asymmetric (X-ray) diffraction conditions (Figure S4, Supporting Information), indicate that along with $\text{MAPbI}_3 \cdot \text{H}_2\text{O}$, also ordered MAPI is present even in the upper layers, within $\approx 200 \text{ nm}$ from the surface, a finding that provides solid evidence for the proposed coexistence of MAPI and $\text{MAPbI}_3 \cdot \text{H}_2\text{O}$.^[23] Additionally, the volume expansion that is indicated from MAPI's diffraction peaks, agrees with a previous finding.^[24] Such expansion of the MAPI lattice is consistent with the presence of intercalated H_2O molecules and, overall, suggests an H_2O gradient of $\text{MAPbI}_3 \cdot x\text{H}_2\text{O}$ with $x = 1$ at the surface to $x = 0$ in the bulk.

To detect any volatile products from the bulk of the sample and get a direct identification of traces of H_2O and other decomposition products (if any), we used TGA/DTA-MS to identify and quantitatively measure the mass of gases evolving from the crystals during their controlled heating (Section II, Supporting Information).

The omni-presence of water in the MS background (from ambient air that enters the TGA chamber and MS column, during sample loading ($< 1 \text{ min}$ in total), and water in the carrier gas, Helium (99.999%)), makes it challenging to differentiate the background water signals from those of the sample, if the latter are very small, relative to the total sample weight. To decrease the level of water (and oxygen) in the MS background as much as possible, the TGA/DTA-MS system is cleaned with high purity Helium (99.999%) for at least 20 h before starting the measurement, and for $\approx 90\text{--}100 \text{ min}$ after sample loading. This careful long cleaning of TGA-MS system (details, Section II, Supporting Information) provided a low water background level (raw Mass spec response in the range of $9 \times 10^{-11}\text{--}2 \times 10^{-10}$ torr) and allows to detect the low MS signal of evolved water from the sample.

As a control sample, a MAPI single crystal (stored in N_2 for 6 days, at $< 10\%$ RH at $22 \text{ }^\circ\text{C}$) was measured and its thermogram

shows a slowly spread mass loss of 0.011% (0.014 mg in absolute mass, considering total mass of 1278 mg) from 40 to $190 \text{ }^\circ\text{C}$ (Figure 2), possibly H_2O from the monohydrate (in XRD, Figure 1a), as no other decomposition products of MAPI are observed. For this sample no H_2O signal above background was detected in the MS.

To equilibrate samples under controlled humidity conditions, an in-house designed N_2 -dry box was built and used (Figure S5, Supporting Information). The relative humidity (RH) is regulated by potassium carbonate (K_2CO_3) salt solutions, and the temperature is held at $24.0 \pm 0.5 \text{ }^\circ\text{C}$, well below the tetragonal to cubic phase change temperature ($42 \text{ }^\circ\text{C}$) of MAPI (details, Section II, Supporting Information).

For a wet sample, the MAPI single crystals (stored till then in N_2 at $< 10\%$ RH at $22 \text{ }^\circ\text{C}$) were exposed to $52 \pm 1\%$ RH at $25 \pm 1 \text{ }^\circ\text{C}$ for 5 days (named as MAPI_Wet_5d). A mass loss of 0.061% (0.078 of 129.3 mg) is observed during heating from 40 to $235 \text{ }^\circ\text{C}$ at a $5 \text{ }^\circ\text{C min}^{-1}$ ramp rate (Figure S6, Supporting Information). Also, for this sample no H_2O MS signal above background could be detected.

The challenge in measuring a very small amount of evolved H_2O vapor from the sample is its significant dilution by the constant flow of carrier gas (He), especially if H_2O vapors are slowly released during heating. The flow of the carrier gas was maintained at 30 cc min^{-1} , the minimum necessary for MS to avoid creating under-pressure in the TGA chamber, but even with this flow no signal could be detected because of the too high dilution. A clear MS signal requires a sharp water release, i.e., weight loss during a relatively short time. During slow release of water (low level of water), its MS signal is masked by the background noise.

To overcome this, one strategy could be to accumulate mass loss (volatiles) over as short a time as possible by using a higher ramp rate ($20 \text{ }^\circ\text{C min}^{-1}$, instead of $5 \text{ }^\circ\text{C min}^{-1}$). However, using a $20 \text{ }^\circ\text{C min}^{-1}$ ramp rate resulted in overshoots and non-uniformity of temperature, and created an instability in the TGA microbalance. This instability increased the noise of the measured signal, thus reducing the sensitivity and the

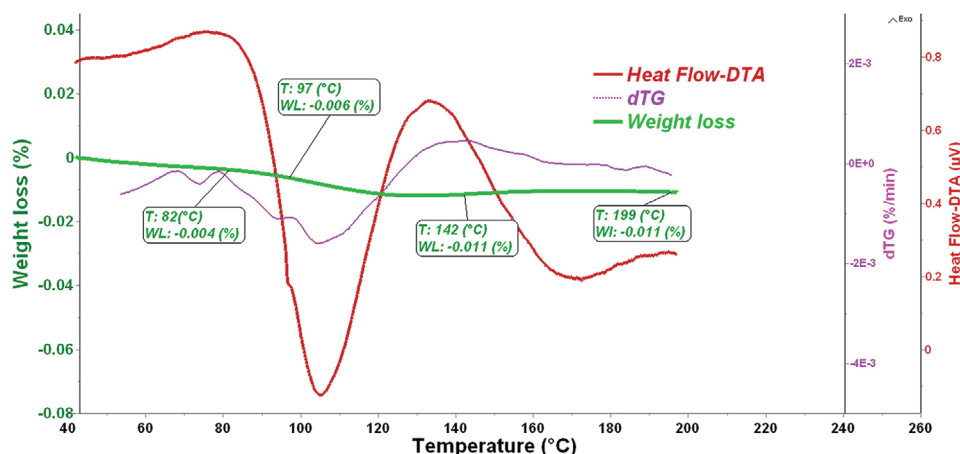


Figure 2. TGA/DTA/DTG spectra of the MAPI control sample, which was, prior to the measurement, stored in N_2 at RH $< 10\%$ and $25 \pm 1 \text{ }^\circ\text{C}$. The thermogram (green, solid curve) is obtained under He flow at a heating rate of $5 \text{ }^\circ\text{C min}^{-1}$. The green (solid) curve represents the weight loss (TGA), pink curve represents the derivative weight loss (dTG-weight loss rate), and the red (solid) curve represents the differential temperature curve -heat flow (DTA).

Table 1. Summary of TGA-MS observations for MAPI_Wet_5d and MAPI_Wet_21d samples.

Sample Name	Mass loss (%) between 86 to 135 °C	H ₂ O MS signal (above background)
MAPI_Wet_5d (Figure S6, Supporting Information)	0.003% (0.004 mg of total mass 129.3 mg)	No
MAPI_Wet_21d (Figure 3)	0.042% (0.052 mg of total mass 125.86 mg)	Yes

reliability of the measurements (Figure S7, Supporting Information). To avoid it, we continued using the 5 °C min⁻¹ ramp rate, that kept the system sufficiently stable to yield reliable measurements and was used throughout the final experiments.

Another strategy to get a clear MS water signal, is equilibrating the samples for longer time in an atmosphere with controlled humidity. We tried this, for 21 days instead of 5, and at 65 ± 1% instead of 52 ± 1% RH (named as MAPI_Wet_21d). As a result, the release of water and its concentration in the carrier gas is now sufficient, so that a significant signal above background could be and was detected. The TGA results of MAPI_Wet_21d show a total mass loss of 0.063% (0.079 mg in absolute mass, considering the total mass = 125.86 mg) from 40 to 235 °C at a 5 °C min⁻¹ ramp rate, similar to that found for MAPI_Wet_5d. However, some striking differences (as shown in Table 1 and Figure 3) were observed in the trend of the thermogram, which present clear and direct evidence of H₂O release from the sample:

1) In the TGA and DTG traces there is a sharp mass loss of 0.042% (0.052 of 125.86 mg) between 86 and 135 °C (well above the temperatures of dehydration of the monohydrate and of release of adsorbed water, at room temperature under dry gas flow)^[9,24]

2) A clear H₂O MS signal is identified (Figure 3)

3) No other decomposition products of MAPI are detected in the MS. That result is consistent with that no visible color changes and no changes in AFM topography after exposure to high humidity were observed (Figure S8 and Figure S12, Supporting Information).

The first reason for the small mass loss values associated with water is that H₂O's molecular weight is <3% of the formula weight of MAPI. Beyond such intrinsic low value, the

very small mass loss that is observed consistently in our measurements (≈0.06%) is an order of magnitude lower than the lowest reported value (0.9%).^[6] One can argue that such a low mass loss is due to long flushing of the TGA chamber after sample loading, during which the water that was adsorbed on the crystal surface and/or that of the monohydrated top layers might be removed and carried away. Leguy et al. report that the hydration content of the monohydrate in MAPbI₃ can be reduced to MAPbI₃·0.15H₂O by drying the crystal in dry air/N₂ (more importantly, just at RT) for 90 min^[9] corresponding to 0.9% in weight, a value an order of magnitude larger than ours. To exclude the effect of the flushing time in our chamber we measured the difference between a long, 90–100 min flush (usual case, unless stated otherwise) and a shorter, 20 min, flush. We found that with the short 20 min flush time, the mass loss of the sample is ≈0.09% (Figure S9, Supporting Information and details for no net H₂O MS signal in this case is described in Section II, Supporting Information), and with the long 90 min flush it is ≈0.06% (Figure 3), between RT and 235 °C. Still, even the maximum mass loss of ≈0.09% in our case is an order of magnitude lower than the lowest reported value (0.9% from TGA, shown in Figure 2 of ref. [6]).

Considering our criteria to detect the water from the near-surface and microns deep into the material, long flushing is crucial to lower the background H₂O, and to enable measuring a clear MS signal from the sample, especially for very small mass loss. Another reason for the small mass losses that we measure can be our use of high-quality single crystals, instead of polycrystalline thin films or powders, used for earlier reports and that the absence of grain boundaries in single crystals results in low (slow) diffusion of water into the bulk. Our result

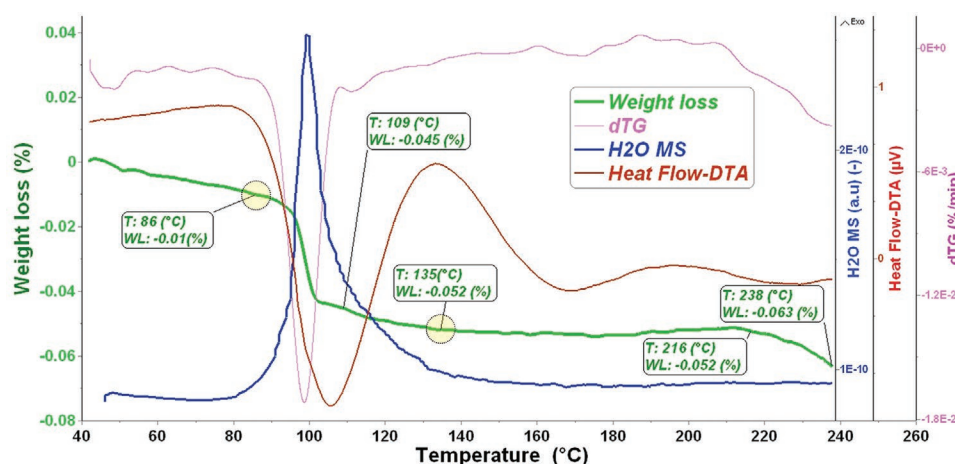


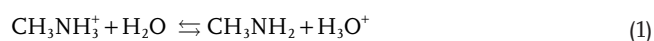
Figure 3. TGA/DTG/DTA-MS spectrum of MAPI_wet_21d sample under He flow at a heating rate of 5 °C min⁻¹, equilibrated for 21 days under 65 ± 1%RH, at 25 ± 1 °C. The green (solid) curve represents the weight loss (TGA), the pink curve represents the derivative weight loss (dTG-weight loss rate), the red (solid) curve represents the differential temperature curve- heat flow (DTA), and the blue (solid) curve represents the MS spectrum of released H₂O (18 amu). The downward peak of the DTA in this profile indicates an endothermic process during the release of water from the MAPI.

is in good agreement with the report that bulk material has higher stability to humidity than surface-rich polycrystalline films,^[25]

To further check if the MS signal of H₂O results from surface adsorption of a H₂O layer or from the bulk, we performed a surface-sensitive experiment by determining the contact potential difference (CPD) using a Kelvin Probe. As a control sample, the (100) surface of a MAPI crystal without monohydrate, as confirmed by XRD (Figure S10, Supporting Information), termed “MAPI_clean” (see Section I, Supporting Information) was measured. The measurement was done after 2 h in dry N₂ in the dark, conditions that are similar to those used for flushing before the TGA-MS experiment, before and after exposure of the single crystal to humid conditions (65 ± 1% RH at 25 ± 1 °C) for 3 days. The work function of the MAPI_clean single crystal is slightly smaller after exposure to humidity, by up to 40 (±10) meV (Figure S11, Supporting Information). This small difference (and its slight decrease with time) is likely due to (removal of) residual adsorbed species at RT. The work function of a MAPI crystal that shows a monohydrate XRD peak (Figure 1a) is over 200 meV higher than that of MAPI_clean and shows the same few tens of meV smaller work function after humidity exposure as MAPI_clean (Figure S11, Supporting Information). The CPD of all samples that we measure is quite stable for >2000 sec (even considering the above-mentioned slight decrease, see Figure S11, Supporting Information), indicating that the crystals do not change during each experiment. Moreover, atomic force microscopy, AFM, images indicate no change in surface topography between the MAPI single crystal surfaces after exposure to high humidity, compared to the same surface at low humidity (Figure S12, Supporting Information). Overall, these results are consistent with that of any H₂O MS signal that is obtained in the TGA-MS experiment, evolves from the bulk.

Additionally, keeping in mind the monohydrate XRD peak (Figure 1a), if we assume that all the mass loss observed in TGA corresponds to H₂O molecules from the ordered monohydrate, i.e., considering a 1:1 H₂O: MAPI ratio, the observed mass loss would correspond to a 2 μm thick monohydrate. This depth we can view as a minimum penetration depth; it would correspond to >1900 monolayers of the crystal (for each face), a very high number, which makes adsorbed water not a relevant interpretation.

Garcia-Fernandez et al. reported that humidity-exposed (polycrystalline) MAPbI₃ exhibited an increase in electrical conductance over dry samples, which is only possible by an increase in the density of electrical charge carriers, i.e., either electrons or ions,^[6] something that can be due to surface transfer doping or water molecules diffusing into the grains.^[26–30] Ceratti et al. deduced that the presence of water molecules in MAPbI₃, at least up to 100 nm from the crystal surface, triggers and drives proton diffusion, something that can be relevant here,^[10] as the H₂O that we detect could have diffused as Hydronium ion (H₃O⁺) by proton exchange with the organic entity, i.e., methylammonium (MA⁺), according to



Based on this mechanism, we assume the diffusion coefficient of water ($D_{\text{H}_2\text{O}}$) to be the same as what was derived for

protons,^[10] i.e., $D_{\text{H}_2\text{O}}$ is taken as $2.4 \times 10^{-8} \text{ cm}^2 \text{ s}^{-1}$ for MAPI at $T = 100 \text{ °C}$, the temperature of the relevant peak of dTG and the corresponding MS signal of H₂O (Figure 3). Our assumption concerning the diffusion coefficient relies on the relatively facile proton diffusion, which is based on both theoretical and experimental results, over the past years, as reported in references.^[31–36] From the suggested diffusion mechanism and from the results of DFT computations of H₂O migration in MAPI,^[12] the possible diffusion path for H₂O molecules in MAPI seems to be by then interacting with the A site cation and moving between unit cells, via empty A sites and/or via the intervening space between the A site and the PbI₆ octahedra (viewed as one of the interstitial sites in static lattice and defect models).

Having in hand direct evidence of release of water from bulk MAPI single crystals, we can estimate, from how deep the water can diffuse through the sample to the surface in the time frame during which the MS signal is observed (10 min). Using the $D_{\text{H}_2\text{O}}$ value, we estimate the water diffuses ≈40 μm in 10 min (Section III, Supporting Information) and we view this as the maximum penetration depth.

In addition, based on the mass loss identification in TGA, we can estimate how many MAPI formula units are associated with each water molecule in the sample. To get this we assume that all the water that is released was uniformly distributed in the measured crystal before the TGA-MS measurement started. Considering the active mass (material that is exposed to water) of MAPI for 40 μm from the surface, we estimate, on an average there are around three formula units of MAPI for each molecule of H₂O, i.e., MAPbI₃·0.33H₂O (Section III, Supporting Information). This estimate agrees well with reports on proton migration and optoelectronic effects in MAPI at concentrations lower than its monohydrate^[6,10] and indicates that the stability of the material is not compromised as, no decomposition products are found with the TGA-MS before the thermal decomposition temperature.

3. Conclusion

We used TGA-MS to show direct evidence of H₂O molecules penetrating several tens of μm into MAPI single crystals when exposed to controlled humidity. While we note that, the dry MAPI single crystal has shown the presence of monohydrate in XRD, we deduce that equilibrating the crystals further under controlled humidity has resulted in diffusion of H₂O into its bulk. Sufficient H₂O accumulated during exposure, making it possible to observe a clear H₂O signal during the TGA-MS experiments. Importantly, we did not observe any decomposition products of MAPI (between RT to 235 °C) despite its interaction with H₂O molecules under Nitrogen. Based on the total water weight loss and assuming uniform distribution, the average concentration of H₂O in the penetrated section of MAPI is MAPbI₃·0.33H₂O. This may be an oversimplification, as our XRD ($(\theta-2\theta)$ and Phi scan) findings indicate a possible combination of MAPI and MAPbI₃·H₂O, suggesting an H₂O gradient of MAPbI₃·xH₂O with $x = 1$ at the surface to $x = 0$ in the bulk. Our finding is important, given that many HaP samples will be exposed to medium humidity conditions between their preparation, characterization and/or inclusion in a

device. For general sample characterization by XRD we recommend that θ - 2θ measurements of HaPs (MAPbI₃) will include scanning to lower 2θ values, i.e., if Cu K α radiation is used, start from 5° instead of the usual 10°, to check for the possible presence of a monohydrate (MAPbI₃·H₂O).

Supporting Information

Supporting Information is available from the Wiley Online Library or from the author.

Acknowledgements

NPJ thanks Dr. Shay Tirosh for technical support and guidance. N.P.J. and D.C. thank Reut Cohen, Michal Weitman for earlier work on this problem at Bar Ilan University, and Drs. Irit Goldian and Sidney Cohen (Weizmann Institute of Science) for the AFM measurements. The authors thank the reviewers for their constructive comments. NPJ acknowledges funding from the European Union's Horizon 2020 MSCA Innovative Training Network MAESTRO under grant agreement no. 764787. Additional support was obtained from the Nancy and Stephen Grand Technion Energy Program (GTEP). G.S.G. acknowledges the support of the Arturo Gruenebaum Chair in Materials Engineering. At Bar-Ilan University work was supported by the Israel Ministry of Energy as part of the Solar ERANet PerDry consortium and at the Weizmann Institute of Science by the Minerva Centre for Self-Repairing Systems for Energy & Sustainability, and the CNRS-Weizmann program.

Conflict of Interest

The authors declare no conflict of interest.

Author Contributions

N.P.J. and G.E.S. contributed equally to this work. DC and NPJ designed this project, discussed the results and calculations. NPJ synthesized and characterized the crystals and set up the humidity exposure experiments. GES and NPJ discussed and designed the TGA-MS measurements. GES performed and GG and GES analyzed the TGA-MS measurements. NPJ and YF performed and analyzed XRD measurements. DRC provided initial stimulus for the project and contributed to the discussions during the project. AK performed the CPD measurements. IB designed the N₂ dry box. DC and GG supervised this work. NPJ wrote the initial draft and finalized it with DC, GG, GES, YF, and DRC.

Data Availability Statement

The data that support the findings of this study are available from the corresponding author upon reasonable request.

Keywords

humidity, MAPbI₃, monohydrate, single crystal quality

Received: April 16, 2022

Revised: July 26, 2022

Published online: August 21, 2022

- [1] S. Kundu, T. L. Kelly, *EcoMat* **2020**, *2*, e12025.
- [2] Z. Song, A. Abate, S. C. Watthage, G. K. Liyanage, A. B. Phillips, U. Steiner, M. Graetzel, M. J. Heben, *Conf. Rec. IEEE Photovolt. Spec. Conf.* **2016**, 1202.
- [3] S. Chen, A. Solanki, J. Pan, T. C. Sum, *Coatings* **2019**, *9*, 535.
- [4] H. H. Huang, Z. Ma, J. Strzalka, Y. Ren, K. F. Lin, L. Wang, H. Zhou, Z. Jiang, W. Chen, *Cell Reports Phys. Sci.* **2021**, *2*, 100395.
- [5] A. Solanki, S. S. Lim, S. Mhaisalkar, T. C. Sum, *ACS Appl. Mater. Interfaces* **2019**, *11*, 25474.
- [6] A. García-Fernández, Z. Moradi, J. M. Bermúdez-García, M. Sánchez-Andújar, V. A. Gimeno, S. Castro-García, M. A. Senaris-Rodríguez, E. Mas-Marzá, G. Garcia-Belmonte, F. Fabregat-Santiago, *J. Phys. Chem. C* **2019**, *123*, 2011.
- [7] G. Grancini, V. D'Innocenzo, E. R. Dohner, N. Martino, A. R. Srimath Kandada, E. Mosconi, F. De Angelis, H. I. Karunadasa, E. T. Hoke, A. Petrozza, *Chem. Sci.* **2015**, *6*, 7305.
- [8] W. Zhou, Y. Zhao, C. Shi, H. Huang, J. Wei, R. Fu, K. Liu, D. Yu, Q. Zhao, *J. Phys. Chem. C* **2016**, *120*, 4759.
- [9] A. M. A. Leguy, Y. Hu, M. Campoy-Quiles, M. I. Alonso, O. J. Weber, P. Azarhoosh, M. Van Schilfgaarde, M. T. Weller, T. Bein, J. Nelson, P. Docampo, P. R. F. Barnes, *Chem. Mater.* **2015**, *27*, 3397.
- [10] D. R. Ceratti, A. Zohar, R. Kozlov, H. Dong, G. Uraltsev, O. Girshevitz, I. Pinkas, L. Avram, G. Hodes, D. Cahen, *Adv. Mater.* **2020**, *32*, 2002467.
- [11] D. R. Ceratti, A. Zohar, G. Hodes, D. Cahen, *Adv. Mater.* **2021**, *33*, 2102822.
- [12] U. G. Jong, C. J. Yu, G. C. Ri, A. P. McMahon, N. M. Harrison, P. R. F. Barnes, A. Walsh, *J. Mater. Chem. A* **2018**, *6*, 1067.
- [13] C. Zheng, O. Rubel, *J. Phys. Chem. C* **2019**, *123*, 19385.
- [14] Q. Li, Z. Chen, I. Tranca, S. Gaastra-Nedea, D. Smeulders, S. Tao, *Appl. Surf. Sci.* **2021**, *538*, 148058.
- [15] R. D. Hoehn, J. S. Francisco, S. Kais, A. Kachmar, *Sci. Reports* **2019**, *9*, 668.
- [16] A. Kakekhani, R. N. Katti, A. M. Rappe, *APL Mater.* **2019**, *7*, 041112.
- [17] E. Mosconi, J. M. Azpiroz, F. De Angelis, *Chem. Mater.* **2015**, *27*, 4885.
- [18] C. Müller, T. Glaser, M. Plogmeyer, M. Sendner, S. Döring, A. A. Bakulin, C. Brzuska, R. Scheer, M. S. Pshenichnikov, W. Kowalsky, A. Pucci, R. Lovrinčić, *Chem. Mater.* **2015**, *27*, 7835.
- [19] E. J. Juárez-Pérez, Z. Hawash, S. R. Raga, L. K. Ono, Y. Qi, *Energy Environ. Sci.* **2016**, *9*, 3406.
- [20] Z. Song, C. Wang, A. B. Phillips, C. R. Grice, D. Zhao, Y. Yu, C. Chen, C. Li, X. Yin, R. J. Ellingson, M. J. Heben, Y. Yan, *Sustain. Energy Fuels* **2018**, *2*, 2460.
- [21] F. Fu, S. Pisoni, Q. Jeangros, J. Sastre-Pellicer, M. Kawecki, A. Paracchino, T. Moser, J. Werner, C. Andres, L. Duchêne, P. Fiala, M. Rawle, S. Nicolay, C. Ballif, A. N. Tiwari, S. Buecheler, *Energy Environ. Sci.* **2019**, *12*, 3074.
- [22] F. Hao, C. C. Stoumpos, Z. Liu, R. P. H. Chang, M. G. Kanatzidis, *J. Am. Chem. Soc.* **2014**, *136*, 16411.
- [23] Z. Song, N. Shrestha, S. C. Watthage, G. K. Liyanage, Z. S. Almutawah, R. H. Ahangharnejhad, A. B. Phillips, R. J. Ellingson, M. J. Heben, *J. Phys. Chem. Lett.* **2018**, *9*, 6312.
- [24] Z. Zhu, V. G. Hadjiev, Y. Rong, R. Guo, B. Cao, Z. Tang, F. Qin, Y. Li, Y. Wang, F. Hao, S. Venkatesan, W. Li, S. Baldelli, A. M. Guloy, H. Fang, Y. Hu, Y. Yao, Z. Wang, J. Bao, *Chem. Mater.* **2016**, *28*, 7385.
- [25] A. M. Askar, G. M. Bernard, B. Wiltshire, K. Shankar, V. K. Michaelis, *J. Phys. Chem. C* **2017**, *121*, 1013.
- [26] M. A. Haque, A. Syed, F. H. Akhtar, R. Shevate, S. Singh, K. V. Peinemann, D. Baran, T. Wu, *ACS Appl. Mater. Interfaces* **2019**, *11*, 29821.
- [27] W. Chen, D. Qi, X. Gao, A. T. S. Wee, *Prog. Surf. Sci.* **2009**, *84*, 279.
- [28] K. J. Rietwyk, D. A. Keller, A. Ginsburg, H. N. Barad, M. Priel, K. Majhi, Z. Yan, S. Tirosh, A. Y. Anderson, L. Ley, A. Zaban, *Adv. Mater. Interfaces* **2019**, *6*, 1802058.

- [29] C. Ma, B. Kim, D. H. Kang, S. W. Kim, N. G. Park, *ACS Energy Lett.* **2021**, *6*, 2817.
- [30] G. N. Hall, M. Stuckelberger, T. Nietzold, J. Hartman, J. S. Park, J. Werner, B. Niesen, M. L. Cummings, V. Rose, C. Ballif, M. K. Chan, D. P. Fenning, M. I. Bertoni, *J. Phys. Chem. C* **2017**, *121*, 25659.
- [31] D. A. Egger, L. Kronik, A. M. Rappe, *Angew. Chem., Int. Ed.* **2015**, *54*, 12437.
- [32] D. A. Egger, A. M. Rappe, L. Kronik, *Acc. Chem. Res.* **2016**, *49*, 573.
- [33] C. Cardenas-Daw, T. Simon, J. K. Stolarczyk, J. Feldmann, *J. Am. Chem. Soc.* **2017**, *139*, 16462.
- [34] S. Sadhu, T. Buffeteau, S. Sandrez, L. Hirsch, D. M. Bassani, *J. Am. Chem. Soc.* **2020**, *142*, 10431.
- [35] Y.-F. Chen, Y.-T. Tsai, L. Hirsch, D. M. Bassani, *J. Am. Chem. Soc.* **2017**, *139*, 16359.
- [36] T. Buffeteau, L. Hirsch, D. M. Bassani, *Adv. Mater.* **2021**, *33*, 2007715.